O environment of unpaired Si bonds (P_b defects) at the (111)Si/SiO_2 interface

A. Stesmans and K. Vanheusden
Department of Physics, Katholieke Universiteit Leuven, 3001 Leuven, Belgium
(Received 29 April 1991; revised manuscript received 24 June 1991)

The immediate oxygen environment in the silica side of the [111]P_b defect (an interfacial $Si\equiv Si_3$ defect with an unpaired sp^3-like hybrid perpendicular to the interface) has been revealed from ^{17}O hyperfine (HF) structure electron-spin-resonance measurements on (111)Si/SiO_2 structures enriched to 51.24% ^{17}O. The results show that the sp^3 hybrid has its strongest HF interaction, characterized by the HF splitting constant $a_{\|1}=2.7\pm0.15$ G, with only one O site in a first shell, a next interaction of $a_{\|2}=1.1$ G with one O site in a second shell, and a third interaction of $a_{\|3}\approx0.2$ G with two equivalent O sites in a third shell. These results complete the model of the P_b defect and conflict with a previously proposed tridymitelike model for the silica side of the P_b defect.

I. INTRODUCTION

Thermal oxidation or nitridation of Si at any temperature T is accompanied by the generation of intrinsic interface defects to relieve interface strain. The dominant defect at the (111) Si/SiO_2 interface is termed the P_b center,[1,2] which accounts for 50–100 % of all electrically active trapping and recombination fast interface states.[3] As these defects degrade device performance, they are a main concern in solid-state-device fabrication, particularly in the light of the ever down-scaling trend of devices. The P_b defect has been identified—mainly by the electron-spin-resonance (ESR) technique—as an unpaired sp^3 orbital on a trivalently bonded interface Si atom pointing into a microvoid.[2,4] It has C_{3v} symmetry and is schematically denoted as $Si\equiv Si_3$. It is noteworthy that only the [111]P_b variant with an unpaired sp^3 hybrid perpendicular to the interface (sketched in Fig. 1) is observed in a conventional as-oxidized (1 atm dry O_2; 900 °C–950 °C) (111) Si/SiO_2 structure.[5,6] Such an interface, typically comprising about 5×10^{12} P_b defects cm^{-2}, is abrupt (extending over only 1 to 3 atomic planes) and atomically smooth over long distances; flat regions of up to about 1000 nm^{-2} are separated by ledges typically 1 to 2 atomic steps high.

The $Si\equiv Si_3$ model accounts for most of the experimental observations on the P_b defect, of which the main properties are primarily set by the Si substrate. Yet this model is incomplete in the sense that it only reflects the Si (substrate) "side" of the defect. A full model of this prototype interface defect, located in the transition plane of a sharply bordered interface, would also incorporate the surrounding structure at the insulator side. That additional insight could provide information on the physical mechanism(s) by which the P_b's are formed.

So far, little is known about the P_b's immediate oxide environment. A preeminent method to map that environment would be the observation of ^{17}O (nuclear spin $I=\frac{5}{2}$) P_b hyperfine (HF) signals in the ESR spectrum, an almost unique method on that matter. There has been one attempt[7] in this direction comparing 20.0-GHz observations at $T\geq20$ K of an (111)/Si/SiO_2 structure grown in ordinary oxygen (0.037% ^{17}O natural abundance) with one enriched to 51.26% ^{17}O. However, this was unsuccessful as the mere effect of ^{17}O enrichment was a broadening of the peak-to-peak linewidth ΔB_{pp} from about 1.4 to 4.2 G, from where it was concluded that O is not incorporated in the immediate bonding structure of P_b. A similar conclusion was reached from a comparative study[8] of Si oxide and nitride showing that the insulator's influence on the P_b ESR features is only of secondary nature.

Recent experiments,[9] however, have led to a more thorough understanding of the P_b signal structure. In particular the dipole-dipole (DD) interaction between P_b's has been identified, mainly as a result of the optimization of a reversible H-passivation method. The natural line shape, that is, the shape unaffected by DD broadening, has been well characterized and a unique $\Delta B_{pp}-[P_b]$ relationship has been revealed. These results show that the P_b concentration is an important parame-

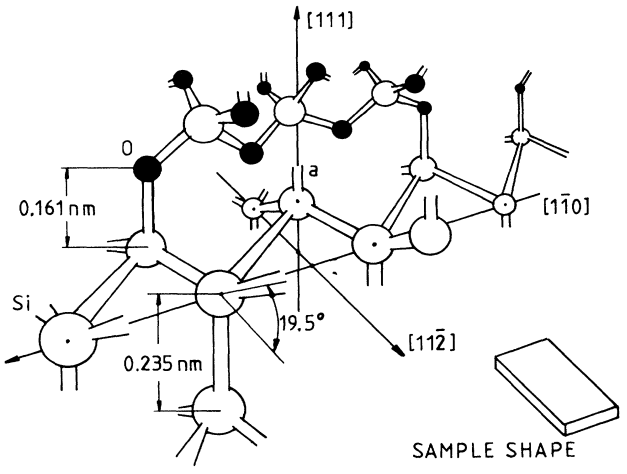

FIG. 1. Sketch of the atomic arrangement at the (111)Si/SiO_2 interface, where entity a represents a [111]P_b defect.

ter and entail that any comparison, either experimental or theoretical and computational, regarding the effect of ^{17}O enrichment must be carried out between otherwise *strictly identical* samples in order to keep $[P_b]$, and thus DD effects, unaltered. In particular, this means that to simulate the P_b spectrum of ^{17}O-enriched Si/SiO_2, the calculated ^{17}O HF histogram has to be convoluted with the correct spectrum of unenriched Si/SiO_2 of *equal* $[P_b]$.[10]

This insight has opened another perspective for ^{17}O P_b measurements. Together with a low-T ESR spectrometry optimized to record clear *undistorted* resonances and well-controlled *reproducible* sample preparation, this has revealed an ^{17}O P_b HF structure. Simulation of this structure based on the calculation of the ^{17}O HF stick diagram for various O shell environments and correct convolution provides information on the immediate O surroundings of the P_b defect.

II. EXPERIMENTAL DETAILS

Slices measuring $0.12\times2\times9$ mm^3 were cut from a commercial Czochralski-grown (111)Si wafer (p type, 10 Ω cm) polished to optical flatness at both sides. After careful cleaning these platelets were oxidized[11] at 920 °C±10 °C either in ordinary oxygen (purity >99.999%) or oxygen enriched to 51.24% ^{17}O at a pressure of 0.2 atm for about 75 min resulting in an oxide thickness of ≈145 Å. Particular attention was paid to cycle both samples fully identically, apart, of course, from the differing O_2 ambient. Post-oxidation thermal treatments in vacuum and hydrogen, as detailed elsewhere,[9] were applied to optimize the P_b density at the balance of a favorable signal-to-noise (S/N) ratio and an acceptable DD broadening. Typically 15 slices were stacked together for ESR measurements. The final P_b density was $(4.9\pm0.3)\times10^{12}$ and $(5.2\times0.5)\times10^{12}$ cm^{-2} for the unenriched and enriched samples, respectively. Note that these are well equal within experimental accuracy as strictly required for the present purpose.

K-band (≈20.1 GHz) ESR absorption-derivative $dP_{\mu a}/dB$ signals ($P_{\mu a}$ representing the absorbed microwave power) were measured at 4.3 K for the applied magnetic induction **B** perpendicular to the (111) interface[12] (**B**‖[111]). The high saturability of the P_b signal at this low T forced us to reduce the microwave power P_μ incident on the TE_{011} cavity of loaded Q of ~15 000 to ≤0.5 nW to record undistorted signals. Signal averaging (typically ≈20 traces) has been applied routinely; digital filtering, however, has not been used.

III. EXPERIMENTAL RESULTS AND INTERPRETATION

A. ESR spectra

The P_b signals of both the unenriched and enriched samples are shown in Fig. 2. The unenriched sample is characterized by $\Delta B_{pp}=1.69\pm0.03$ G and a line-shape factor $\kappa\equiv I/[V_D(\Delta B_{pp})^2]=5.6\pm0.3$, where I and $2V_D$ represent the signal intensity (area under the integrated derivative spectrum), and peak-to-peak height of the $dP_{\mu a}/dB$ signal, respectively. The corresponding density $[P_b]=(4.9\pm0.3)\times10^{12}$ cm^{-2} refers[9] to a DD broadening of 0.4 G. The distinct effect of ^{17}O enrichment is clear from a comparison of both spectra showing a broadening of the P_b response to $\Delta B_{pp}=2.71\pm0.06$ G. More exciting, however, is the appearance of (partially) resolved ^{17}O HF structure, which has three main characteristics as indicated in Fig. 2(a): a kink at position A, a resolved peak at B, and a broadly extending shoulder indicated[13] as region C. These features may serve as clues to interpret the effect of enrichment in terms of the O environment. The increase of the line-shape factor for the enriched sample to 10.1±0.8 just confirms the appearance of the additional structure.

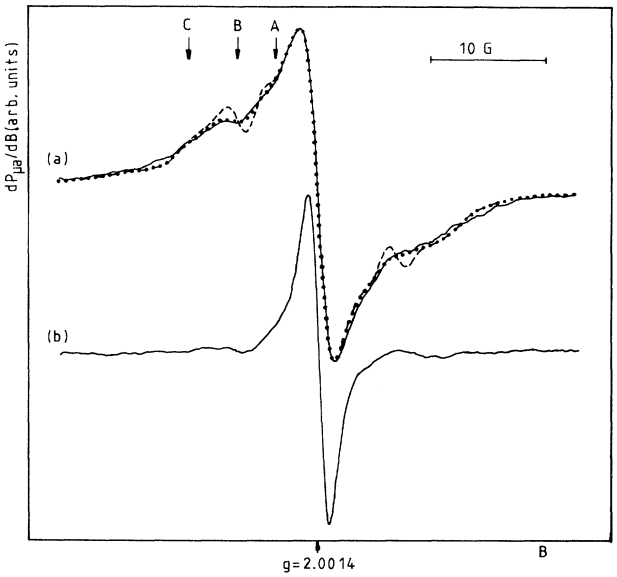

FIG. 2. K-band (20.1-GHz) ESR spectra (solid curves) of the [111]P_b defect measured at 4.3 K with $P_\mu=-65$ dBm and **B**⊥(111) interface on (111)Si/SiO_2 grown in oxygen enriched to 51.24% ^{17}O(a) and ordinary oxygen (b), corresponding to a P_b density of $(5.2\pm0.5)\times10^{12}$ and $(4.9\pm0.3)\times10^{12}$ cm^{-2}, respectively. The arrows indicate characteristic features resulting from ^{17}O P_b HF interaction. The dashed curve is a computer simulation based on ^{17}O HF histogram calculation using the parameters summarized in Table I. The dotted curve, representing the optimum fit, is derived from the dashed curve by adding spreads in $a_{\|i}$ as given in Table I also.

It should be noted that the observed structure in Fig. 2(a) after ^{17}O enrichment does not result from the weak structure resolved in the unenriched sample spectrum [Fig. 2(b)]. As shown elsewhere, the latter structure results from a ^{29}Si superhyperfine and a fine structure (DD) doublet.[9] And, when carrying out an ^{17}O enrichment, each such doublet line is, similar to the central line, strongly broadened by the ^{17}O histogram. In the light of the relative intensities involved, this results in a total fading of the weak structure in the enriched sample spectrum as compared to the central signal. The latter now

predominantly reflects the ^{17}O interaction.

It is clear that the observed ^{17}O HF splittings are much smaller than that resulting from HF interaction with a central ^{29}Si nucleus (isotropic HF splitting ≈ 156 G),[4] as anticipated by the fact that, unlike Si, oxygen is not an immediate part of the P_b structure.

B. Spectra simulation and interpretation

Simulation of the P_b signal of the enriched sample starts from the calculation of the HF spectral histogram for the configuration of a P_b defect that is surrounded by r shells each containing n_i *equivalent* O sites, where $r=4$ and $n_i=0,\ldots,10$. Each O site has a probability $p=0.5124$ for being occupied by an ^{17}O atom. Such a histogram is simply obtained by accumulating the shifts in resonance field caused by each surrounding ^{17}O nucleus *individually* and the corresponding statistical amplitude for each "line" (stick). This histogram is then convoluted with the "unenriched" experimental spectrum of Fig. 2(b) to obtain a simulation.

The simulation task now consists in calculating the convoluted HF histogram for each (physically reasonable) shell configuration, that is, each set of n_1,n_2,n_3,n_4 values, and selecting the best fit. Since it is anticipated[7] that O is not an immediate part of the P_b bonding structure, ^{17}O atoms in more distant shells are expected to cause only small, hardly resolvable HF splittings. Hence the number of shells (r) considered is limited to 4.

The histogram $H(B)$ for one n_1,n_2,n_3,n_4 shell configuration is the accumulation of all pairs

$$H(B)=\left\{\prod_{i=1}^{4} 6^{-k_i} P_{k_i}^{n_i}, B_0+\sum_{i=1}^{4}\sum_{j=0}^{k_i} M_{I,j}a_{\|i}\right\}, \tag{1}$$

where

$$P_{k_i}^{n_i}=\frac{n_i!}{k_i!(n_i-k_i)!}p^{k_i}(1-p)^{n_i-k_i}. \tag{2}$$

$M_{I,0}\equiv 0$ and k_i and $M_{I,j}$ $(j>0)$ are understood to run through all values $0, 1, \ldots, n_i$ and $-\frac{5}{2}, -\frac{3}{2}, \ldots, \frac{5}{2}$, respectively, to cycle all possible combinations. B_0 represents the ESR resonance field in the absence of HF interaction while $a_{\|i}$ is the HF splitting constant for $\mathbf{B}\|[111]$ resulting from interaction of the unpaired P_b sp^3 hybrid with ^{17}O nuclei in shell i. The buildup of the histogram is clear when realizing that a single line (stick) in the histogram is split in six lines of equal intensity—each shifted by $M_I a_{\|i}$—corresponding to the $M_I=-\frac{5}{2},\ldots,\frac{5}{2}$ values of the z component of nuclear spin when interacting with one ^{17}O nucleus in shell i.

The best fitting result is shown in Fig. 2 by the dashed curve, while the corresponding fitting parameters are summarized in Table I. Interestingly, this reveals that the P_b unpaired electron has its strongest HF interaction with only one O site (shell 1) characterized by $a_{\|1}=2.7$ G, which has a probability $p=0.5124$ of being occupied by an ^{17}O nucleus. The second strongest HF interaction is again only with one O site (shell 2) of $a_{\|2}=1.1$ G, while the third-level interaction is with two equivalent O sites in shell 3. The fourth-level HF interaction, of $a_{\|4}\approx 0.1$ G, with 10 equivalent O sites is to be seen as indicative rather than as a correct physical result. The essential point for this shell is that it contains a *large* number of almost equivalent O sites of *small* HF interaction when occupied by ^{17}O atoms. They, in fact, represent the distant hemispherical cloud of small-$a_{\|i}$ O sites of which the mere effect is to slightly blur (broaden) the spectrum. Incorporation of this "shell" only improves slightly the overall fitting quality, but is not essential.

TABLE I. ^{17}O HF splitting data and shell distributions of O sites in the immediate oxide neighborhood of [111]P_b centers in (111)Si/SiO_2 as obtained by fitting 20.1-GHz ESR spectra measured at 4.3 K for $\mathbf{B}\|[111]$.

Shell No.	n_i	$a_{\|i}$ (G)	$\Delta a_{\|_i}=\sigma_{M_I,i}/(2\|M_I\|)$ (G)
1	1	2.7±0.15	0.60
2	1	1.1±0.1	0.25
3	2	0.2	
4	10	0.1	

Though satisfactory, the fit is not yet perfect. It appears still somewhat too "peaky" although it accounts well for all characteristic details of the experimental spectrum [cf. features A, B, and C in Fig. 2(a)] indicating the correctness of the underlying physical model.

The final, almost perfect fit, as shown by the dotted curve in Fig. 2, is obtained by additionally incorporating a spread in $a_{\|i}$, which fades the "peaky" structure. Such spread is known to exist[4,5,14] as a result of the interface strain and/or randomness of the overlaying SiO_x film. This causes slight variations in the positions of the surrounding O sites from P_b site to P_b site, even within one shell, with attendant alterations in wave-function overlap and HF interaction strengths. The spread in $a_{\|i}$ has been incorporated by replacing each line (stick) in the histogram shifted over $M_I a_{\|i}$ by a Gaussian distribution of equal intensity and standard deviation $\sigma_{M_I,i}=2|M_I|\Delta a_{\|i}$, that is, a relative spread of $2|M_I|\Delta a_{\|i}/(2|M_I|a_{\|i})=\Delta a_{\|i}/a_{\|i}\approx 22\%$. Note the increasing impact of $\Delta a_{\|i}$ with increasing field shift.

The physics behind the successful fit is clear. The main HF interaction with one ^{17}O atom in shell 1 leads to six signals of which the $|M_I|=\frac{5}{2}$ and $\frac{3}{2}$ signals account for features B and A in Fig. 2, respectively. The $|M_I|=\frac{1}{2}$ signal mixes with the strong unshifted or slightly shifted central part, thus contributing to a broadening of the line from 1.69 to 2.71 G. The second-level interaction accounts mainly for the broad shoulders (feature C in Fig. 2), while levels 3 and 4, as already mentioned, add to the broadening and blurring of the P_b spectrum.

It needs to be mentioned that, regarding the number of O sites in the first two surrounding O shells, the fit is unique. No reasonable fit can be produced if allowing more than one equivalent O site in the first or second shell. Depending on one's view, this may come as a surprise, particularly in light of the attractive ditrigonal

ring-cap model. This model, proposed as a reasonable means of terminating the Si lattice at a P_b site, accepts a microvoidlike structure for the SiO_2 cap overlaying the P_b defect and pictures the oxide side as a symmetric puckered ditrigonal ring of six SiO_4 tetrahedra. Detailed quantum-mechanical calculations, allowing for spin-polarization effects, have been carried out on a $Si_{22}H_{21}/Si_6O_{18}H_6$ cluster incorporating such a structure, leading to quantitative predictions of the P_b HF tensors describing the interactions with ^{29}Si and ^{17}O atoms in the cluster. Along this axial microvoid model, one expects three equivalent O sites in a first-neighbor (hemispherical) shell, six other equivalent sites in a second more remote shell, and three again in a third shell. However, the uniqueness of the fitting in Fig. 2 regarding the number of equivalent O sites in the first two surrounding shells, or, put differently, the inappropriateness of the *axial* ditrigonal ring model, is demonstrated in Fig. 3. Here are illustrated fittings to the experimental curve for various $a_{\|i}$ values, accepting as onset three equivalent O sites in a first shell. The fittings have been "optimized," to match either the linewidth of the main central signal or the apparent structure in the experimental spectrum, revealing a strong discrepancy. This should not come as a surprise in light of the previously mentioned physics behind the successful fit realized in Fig. 2.

An interesting result of this analysis is that, similar to the Si side, the immediate oxide side of the P_b center reproduces very well from P_b site to P_b site, at least in what concerns the first three surrounding shells. This opposes a random matching of SiO_x to *c*-Si and is in favor of a kind of *epitaxial* transition.[15,16]

Another interesting result is that the relative spread

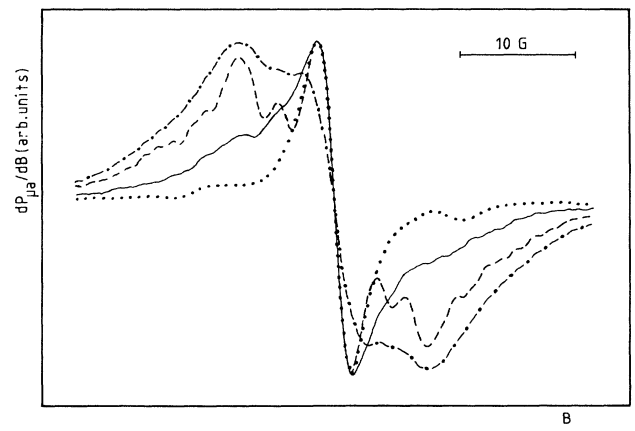

FIG. 3. Fittings of the experimental *K*-band ESR spectrum of the [111]P_b defect (solid line, same as shown in Fig. 2) based on ^{17}O HF histogram calculations accepting as onset three equivalent O sites in a first (strongest HF interaction) neighboring shell in the SiO_2 overlay. The values $a_{\|1}=0.4$ and 2.7 G were used for the dotted and dashed curves, respectively, while for both curves $a_{\|2}=0.1$ G and $n_2=6$. The dash-dotted curve corresponds to $a_{\|1}=2.7$ G, $a_{\|2}=0.8$ G, and $n_2=3$. Similar to the fit in Fig. 2, all three simulations have incorporated a relative spread $\Delta a_{\|i}/a_{\|i}$ in $a_{\|i}$ of $\approx 22\%$.

$\Delta a_{\|}/a_{\|}$ in HF interactions is significantly larger for ^{17}O nuclei, that is $\approx 22\%$, than for central ^{29}Si atoms,[4] for which $\Delta a_{iso}/a_{iso} \approx \Delta a_{\|}/a_{\|} \approx 9.5\%$, where a_{iso} is the isotropic part of the HF interaction. This is as expected since the *c*-Si side of the P_b defect is a much more rigid structure than the oxide side: the Si—O—Si bond angle is much more flexible[17] than the rigid tetrahedral Si—Si—Si angle, which means that the interfacial strain will be largely adapted by the overlaying SiO_2.

IV. DISCUSSION

So far, most HF data on defects have been interpreted along the simplified localized-hybrid-orbital (LHO) picture (see, e.g., Refs. 4 and 18). Within this model the present data regarding the immediate O environment of P_b indicate that the defect has only one O atom in a nearest position, one O atom at a slightly larger distance, two equivalent O atoms in a third-neighbor shell, and many more O atoms in more remote shells. As pointed out previously,[16] however, the LHO model ignores spin-polarization effects of atomic cores by valence levels which makes the model more interpretative rather than predictive. Hence, it is not necessarily so that the O site leading to the strongest ^{17}O HF interaction is also the O site *nearest* to the core of the P_b defect, etc. Yet, the interpretation *is* conclusive about the "symmetry" of the O surrounding, that is, the strongest HF interaction with *only one* O site, closely followed by a weaker HF interaction again with *only one* O site.

The measured ^{17}O HF interaction strengths confirm the previous insight that O is not part of the central bonding structure of P_b, which points to a microvoidlike structure of the SiO_2 cap overlaying the P_b defect. As mentioned, there is so far one such model[16]—an axial microvoid model—which suggests that the first interfacial oxide layers form, in fact, an epitaxial tridymitelike crystalline transition.[15,16] Symmetry considerations, however, show that our results conflict with this otherwise attractive model, which appears to be in line with results of recent simulations of DD-broadened ESR spectra. There are various ways to interpret this finding.

In one, still accepting the basic correctness of the tridymitelike concept, the results could perhaps refer to a distorted symmetry of the six-membered SiO_4 ring cap; if this ring would be off center, for example, this would indeed result in the removal of the axial symmetry of the ^{17}O P_b HF interaction. Previously equivalent O sites could then lead to (slightly) different ^{17}O P_b HF interaction strengths, which would be more in agreement with observations. A difficult to meet requirement for such a modified tridymitelike model, however, might be that, along the present results, the distortion introduced should reproduce largely identically over the numerous P_b sites.

Another interpretation could conclude the inappropriateness of the tridymitelike ring cap thus bearing out the need for another microvoid model. Along one suggestion, the data could well be in line with a matching zigzag overlay consisting of three fairly linearly arrayed SiO_4 tetrahedra, as pictured in Fig. 1. A slight asymmetric re-

laxation of this array resulting in an asymmetric positioning of two O atoms nearest to the P_b core would well agree with the presently deduced ^{17}O HF interactions for the first two "shells." It is realized though that the confirmation of such a model will require an in-depth analysis of the *global* c-Si/SiO_2 matching within the framework of the correct oxidation mechanism.

It should be mentioned that, regarding the magnitude of the largest ^{17}O P_b HF interaction, the present result and the theoretical prediction by the ditrigonal ring-cap model, i.e., $|a_{\|i}|=2.7\pm0.15$ and 2.93 G, respectively, are remarkably similar. This, however, is a trivial result within the concept of a microvoid model for the SiO_2 P_b cap, rather than providing any evidence for the correctness of the tridymitelike model (which is also a microvoid model). Over the various microvoid models, where O is no immediate part of the P_b structure, the ^{17}O HF interaction strengths will be comparable.

It is clear that the correct evaluation of the present results in terms of deriving the correct oxide side of the P_b cluster will require substantial additional theoretical work, starting from detailed quantum-mechanical calculations on those microvoid cluster models which are deemed appropriate. The comparison of the derived symmetry and ^{17}O P_b HF interaction strengths with experiment will then select the correct terminating Si cap overlaying the P_b defect. Such symbiotic interaction of theory and experiment is badly needed to arrive at the model since ESR can only measure interaction symmetries and strengths—not positions of individual atoms.

V. CONCLUSIONS

Optimized ESR measurements on [111]P_b defects in ^{17}O enriched (111)Si/SiO_2 structures have revealed the shell symmetry of O sites in the immediate silica environment. The strength of the ^{17}O HF interactions indicates that O is not incorporated in the central bonding structure of the P_b defect, as expected. A main result is that, regarding the ^{17}O P_b HF interaction, the unpaired P_b electron has its strongest interaction with only one O site in a first shell in the SiO_2 overlay, the next strongest interaction with one O site in a second shell, while the third-level interaction is with two equivalent O sites in shell 3. These data, apparently, conflict with the axial microvoid model based on the concept of the ditrigonal ring SiO_2 cap of P_b.

If the P_b's are seen as somehow coestablishing the intrinsic Si/SiO_2 interface structure rather than being loose results of interface adaptation,[19] the present insight may help reveal this structure and the closely linked oxidation mechanism. This is the ultimate aim and much is expected from cluster-model calculations of the P_b defect incorporating this insight.

[1]Y. Nishi, Jpn. J. Appl. Phys. **10**, 52 (1971).
[2]E. H. Poindexter, P. J. Caplan, B. E. Deal, and R.R. Razouk, J. Appl. Phys. **52**, 879 (1981).
[3]G. J. Gerardi, E. H. Poindexter, P. J. Caplan, and N. M. Johnson, Appl. Phys. Lett. **49**, 348 (1986); S. T. Chang, J. K. Wu, and S. A. Lyon, *ibid.* **48**, 662 (1986).
[4]K. L. Brower, Appl. Phys. Lett. **43**, 1111 (1983).
[5]K. L. Brower, Phys. Rev. B **33**, 4471 (1986).
[6]A. Stesmans, Appl. Phys. Lett. **48**, 972 (1986).
[7]K. L. Brower, Z. Phys. Chem. Nue Folge **151**, 177 (1987).
[8]A. Stesmans and G. Van Gorp, Phys. Rev. B **39**, 2864 (1989).
[9]A. Stesmans and G. Van Gorp, Phys. Rev. B **42**, 3765 (1990); Solid State Commun. **74**, 1003 (1990).
[10]Since the natural abundance of ^{17}O is only 0.037%, there is essentially no ^{17}O HF interaction in a Si/SiO_2 structure grown in ordinary oxygen.
[11]Both oxides were actually grown sequentially on the same lot of slices, starting with the oxidation in ordinary oxygen. After ESR analysis, this oxide was removed in diluted HF upon which the ^{17}O enriched oxide was grown.
[12]The **B**||[111] orientation is imperative for HF structure resolution and optimum signal-to-noise ratio. The P_b resonance is known to broaden considerably as **B** rotates away from [111] thus fading all structure (cf. Refs. 5 and 14). This has prevented to determine $a_{\perp i}$ and, hence also, to separate the isotropic and anisotropic parts of the ^{17}O HF interaction (cf. Ref. 18).
[13]It is a general characteristic that any structural features of the low-T P_b signal are more prominent on the low-field half of the spectrum (see, e.g., Refs. 7 and 9)—possibly related to the slight typical asymmetry for **B**||[111] (see, e.g., Refs. 5 and 14). Hence the present discussion of the characteristic features focuses on the low-field half of the spectrum. It is required, though, that any simulation of the P_b signal should fit the *whole* spectrum, as realized in Fig. 2(a). This just bears out the consistency in combining the correct "unenriched" P_b signal with the correct histogram for the P_b signal on ^{17}O enriched (111)Si/SiO_2.
[14]A. Stesmans and J. Braet, in *Insulating Films on Semiconductors,* edited by J. J. Simone and J. Buxo (North-Holland, Amsterdam, 1986), p. 25.
[15]A. Ourmazd, D. W. Taylor, J. A. Rentschler, and J. Bevk, Phys. Rev. Lett. **59**, 213 (1987).
[16]M. Cook and C. T. White, Phys. Rev. B **38**, 9674 (1988).
[17]A. G. Revesz and G. V. Gibbs, in *Proceedings of the Conference on the Physics of MOS Insulators,* edited by G. Lukovsky, S. T. Pantelides, and F. L. Galeener (Pergamon, New York, 1980), p. 92.
[18]G. D. Watkins and J. W. Corbett, Phys. Rev. **134**, A1359 (1964); A. H. Edwards, Phys. Rev. B **36**, 9638 (1987).
[19]A. Stesmans and G. Van Gorp, Appl. Phys. Lett. **57**, 2663 (1991).